Clin Orthop Relat Res (2010) 468:2410–2418
DOI 10.1007/s11999-010-1283-y

CLINICAL RESEARCH

Morphologic Evaluation of Chronic Radial Head Dislocation

Three-dimensional and Quantitative Analyses

Kunihiro Oka MD, Tsuyoshi Murase MD, Hisao Moritomo MD, Kazuomi Sugamoto MD, Hideki Yoshikawa MD

Received: 20 August 2009 / Accepted: 16 February 2010 / Published online: 4 March 2010

Abstract
Background Treatment of chronic radial head dislocation is controversial, considering whether to reduce and reconstruct the proximal radioulnar joint. The anatomic alteration that influences the decision to reduce the dislocation is not completely understood.
Questions/purposes We attempted to clarify the changes of the proximal radioulnar joint that occur in chronic radial head dislocations to clarify how they might influence the decision to perform repair.
Patients and Methods We evaluated 15 patients with chronic radial head dislocations categorized by duration of "early" (< 3 years) (n = 8) and "longstanding" (> 3 years) (n = 7) groups. We measured the angle and depth of the radial notch of the proximal ulna and evaluated radial head deformity using 3-D bone models created from CT data.
Results For the early group, no differences were observed in the shape of the radial notch between affected and normal sides. For the longstanding group, the radial notch angle was greater on the affected side (mean ± SD, 45.5° ± 9.7°) than on the normal side (29.7° ± 6.3°), and the radial notch depth was smaller on the affected side (0.2 ± 1.6 mm) than on the normal side (2.3 ± 1.3 mm). The shape of the radial head was nearly normal in the early group, whereas the longstanding group had a dome-shaped deformity.
Conclusions In longstanding chronic radial head dislocation, deformation develops in the radial head and radial notch of the ulna, which is remodeled in a manner corresponding to the dislocated position of the radial head.
Level of Evidence Level III, prognostic study. See Guidelines for Authors for a complete description of levels of evidence.

One of the authors (TM) has received funding in support of this research from JST (Japan Science and Technology Agency).
Each author certifies that his or her institution approved the human protocol for this investigation, that all investigations were conducted in conformity with ethical principles of research, and that informed consent for participation in the study was obtained.

K. Oka (✉), T. Murase, H. Moritomo, H. Yoshikawa
Department of Orthopaedic Surgery, Osaka University Graduate School of Medicine, 2-2, Yamada-oka, Suita, Osaka 565-0871, Japan
e-mail: oka-kunihiro@umin.ac.jp

K. Sugamoto
Department of Orthopaedic Biomaterial Science, Osaka University Graduate School of Medicine, Osaka, Japan

Introduction

Treatment for chronic radial head dislocation is controversial; nonoperative treatment has been recommended [19, 24]. Open reduction of the radial head along with ulnar osteotomy [8, 11, 12, 15, 18, 21, 30] and reconstruction of the annular ligament [4, 6, 7, 15, 24, 27, 28] have been attempted to maintain congruity of the radiocapitellar joint because prolonged radial head dislocation leads to long-term complications, such as cubitus valgus deformities [6, 10, 17], osteoarthritis [15, 21, 22], and posterior interosseous nerve palsy [2, 14, 23]. However, the surgical outcome was less satisfactory for longstanding cases [9, 11, 15, 16, 21, 22, 24, 31, 32], and previous studies have revealed reduction of the radial head led to inferior clinical results more than 6 years postinjury [29, 32]. Surgical indications for chronic radial head dislocation have been based on radiographic appearances of overgrowth and changes in convexity of the radial head, and on deformities in the humeral capitulum [11, 15, 21, 31, 32], but little attention has been paid to the morphologic features of the proximal radioulnar joint (PRUJ), which is considered quite important for reducing the radial head to the correct position. We believe the anatomy and pathologic changes of the PRUJ in chronic radial head dislocation should be understood and incorporated in the surgical decision-making process.

The morphologic features of the radial notch in chronic radial head dislocation have not been reported presumably because of the difficulty in evaluating them on plain radiographs. Additionally, previous reports have referred only to the radiographic changes in appearance [11, 21, 22, 24, 31, 32] but not the 3-D size and shape of the radial head, which are crucial for radiocapitellar and radioulnar congruity. In this study, our aim was to observe the morphologic changes of the radial notch of the ulna between affected and unaffected elbows in early- versus longstanding dislocations using 3-D computer bone models created from CT data. Our second aim was to document the altered morphologic features of the radial head, the other component of the PRUJ using these 3-D models.

Patients and Methods

We studied 16 consecutive patients with chronic radial head dislocations who were examined at our institution from December 2002 to December 2007. The inclusion criterion for this study was traumatic radial head dislocation of more than 6 months from the time of initial trauma. Exclusion criteria were acute dislocation of less than 6 months and no obvious traumatic history of the elbow. Among these patients, one with bilateral dislocation with no obvious traumatic history was excluded because the condition was considered congenital [20]. Therefore, 15 patients with traumatic radial head dislocations participated in this study (Table 1). Patients included nine males and six females with an average age of 13 years (range, 4–38 years). Informed consent for participation in this study was obtained from all patients or their guardians as appropriate.

Among the patients studied, 13 had radial head dislocations accompanied by major trauma (fractures of the forearm bones or distal humerus), whereas the other two (Patients 10 and 11) had minor trauma. The two patients with minor trauma had unilateral radial head dislocations and the ulna on the affected side showed extension deformity, which indicated traumatic bowing of the ulna. The mean time elapsed since the initial trauma was 6 months or more, and the mean period from initial injury to examination was 64 months (range, 6–372 months). Among the patients with major trauma, 12 had Monteggia lesions with ulnar fractures or fractures of the radius and ulna, which were classified as Type I (fracture of the ulna with anterior angulation and anterior dislocation of the radial head) (n = 7), Type III (fracture of the ulna with anterior angulation and lateral or anterolateral dislocation of the radial head) (n = 1), and Type IV (fracture of the ulna and radius and anterior dislocation of the radial head) (n = 4), according to the Bado classification [3]. The other major traumatic case (Patient 15) was a supracondylar fracture of the humerus, along with anterior dislocation of the radial head. Of the 13 patients with major trauma, 10 were managed by closed reduction and cast immobilization, two received percutaneous pinning with Kirschner wires, and one underwent open reduction and internal fixation at the initial treatment. The two patients with minor trauma (Patients 10 and 11) had experienced sprains of the elbow 130 and 39 months earlier, respectively. They stated their affected elbows had been swollen and painful for 3 or 4 weeks but had been left untreated at the time of initial injury. In two (Patients 1 and 2) of the four patients with Type IV Monteggia lesions, the radial head was reduced with the forearms supinated, but clicking and anterior dislocation of the radial head occurred in the pronated position. In the remaining 13 patients (11 with major trauma and two with minor trauma), the radial head was dislocated through the entire range of forearm rotation. Among the patients studied, the radial head dislocated anteriorly in 14 and anterolaterally in one (Patient 5).

Previous studies have indicated the radial head becomes misshapen and overgrown within 3 years after injury and congruent proximal radioulnar and radiocapitellar reduction after this time is difficult [16, 24, 31, 32]. Therefore, we classified the 15 patients into two groups based on dislocation duration. Patients who had sustained injury during the previous 3 years were assigned to the “early group” (n = 8). Those who had sustained injury more than 3 years earlier (and those with minor trauma) were assigned to the “longstanding group” (n = 7). Average duration of dislocation was 16.3 months (range, 6–26 months) for the early group and 119 months (range, 38–372 months) for the longstanding group. The average age of the patients at the time of injury was 9.9 years (range, 3–16 years) in the early group and 5.3 years (range: 4–8 years) in the longstanding group. In the early group, one patient (Patient 4) felt pain in the elbow during normal daily activities. Five of the remaining eight patients reported mild pain while playing sports or applying load to the elbow. The other two patients felt no pain in the elbow. Restricted rotation of the forearm was observed in four patients, and the average ranges of pronation and supination were 62° and 73°, respectively. One patient (Patient 3) had difficulty washing her face and receiving a coin in her open palm because of restricted forearm supination. The

Table 1. Patient data summary

Patient	Affected side	Gender	Age at initial injury (years)	Age at examination (years)	Time from injury to examination (months)	Initial injury	Monteggia type	Initial treatment	ROM (pronation/supination) (°)	Chief complaint
Early group										
1	Left	Female	7	9	24	Fx (R & U)	IV	Cast	90/80	Mild pain
2	Right	Male	12	14	21	Fx (R & U)	IV	Cast	90/90	Mild pain
3	Left	Female	13	15	26	Fx (R & U)	IV	Cast	60/0	RFR
4	Left	Male	12	13	6	Fx (R & U)	IV	Pinning	45/50	Moderate pain
5	Left	Female	3	4	14	Fx (U)	III	Cast	90/90	Deformity
6	Left	Male	8	9	8	Fx (U)	I	Cast	60/90	RFR
7	Left	Female	16	17	10	Fx (U)	I	ORIF	60/−30	RFR
8	Left	Male	8	10	21	Fx (U)	I	Cast	90/90	Mild pain
Average			9.9	11.4	16.3				73/58	
Longstanding group										
9	Right	Male	5	14	108	Fx (U)	I	Cast	90/90	Mild pain
10	Right	Male	8	19	130	Elbow sprain			90/90	Mild pain
11	Left	Female	4	7	39	Elbow sprain			90/90	Mild pain
12	Right	Male	5	8	38	Fx (U)	I	Cast	90/90	Mild pain
13	Right	Female	4	11	86	Fx (U)	I	Pinning	90/90	Mild pain
14	Right	Male	7	38	372	Fx (U)	I	Cast	90/90	PIN palsy
15	Right	Male	4	9	59	Fx (DH)		Cast	80/90	Deformity
Average			5.3	15.1	119				88/90	

Fx = fracture; R = radius; U = ulna; DH = distal humerus; ORIF = open reduction and internal fixation; RFR = restricted forearm rotation; PIN palsy = posterior interosseous nerve palsy.

writing and keyboard typing abilities of one patient (Patient 7) were impaired because of restricted forearm pronation. One patient (Patient 5) had no pain and exhibited a full range of forearm rotation but was concerned about elbow deformity.

In the longstanding group, one patient (Patient 14) had posterior interosseous nerve palsy develop but had no elbow-related complaints. Five of the remaining seven patients reported mild pain when playing sports or applying load to the elbow. The remaining felt no pain in the elbow but noticed the projecting radial head. Restricted range of forearm rotation was not observed in patients in the longstanding group.

Both forearms, from elbow to wrist, were scanned in the maximum supinated position using CT (scan time, 0.5 seconds; slice thickness, 0.625 mm; 10 mA, 120 kV) (LightSpeed Ultra16; General Electric, Waukesha, WI). Forearms were fixed on the CT table using a bandage, with the patient prone and arms elevated over the head. Data were saved in digital imaging and communications in medicine format and sent to a computer (Dell Precision™ Workstation 650, 266 MHz/2G; Dell Inc, Round Rock, TX).

Contours of the radius, ulna, and humerus were segmented semiautomatically on the computer. 3-D surface models were constructed based on 3-D surface generation of bone cortex [25] using a visualization toolkit-based original computer program (VTK; Kitware Inc, Clifton Park, NY). We completed surface models of the bilateral humerus, ulna, and radius by deleting the bone marrow data.

To assess the morphologic features of the radial notch of the proximal ulna, we created a mirror image of the 3-D computer model of the contralateral normal ulna, which subsequently was superimposed on the proximal part of the 3-D model of the affected ulna based on the shape of the olecranon and trochlea using the iterative closest point (ICP) registration algorithm, which is one of the most advanced techniques for surface-based registration [1, 5] for comparative assessment of morphologic features (Fig. 1). The ICP algorithm is an iterative alignment algorithm used to (1) establish correspondence between pairs of features in the two structures that are to be aligned based on proximity, (2) estimate transformation parameters using a mean square cost function, and (3) apply that transformation to all features in the first structure. These three steps then are reapplied until convergence is concluded.

To quantify change in the morphologic features of the radial notch, radial notch angle (RNA) and radial notch depth (RND) were defined as follows. First, the ulnar axis with minimal moment of inertia was computed using 3-D ulnar volume data, and the cross-sectional plane of the ulna (plane-U) was determined at the midpoint of the PRUJ perpendicular to the ulnar axis [26] (Fig. 2A). RNA was defined as the angle between Line X (straight line connecting both ends of the radial notch) and Line Y (line made from the ulnar posterior border to the tip of the coronoid process of the normal side, found in the ulnar cross section) (Fig. 2B). RND was the distance between the bottom of the radial notch and Line X (Fig. 3). Changes to the radial head were evaluated by the appearance and size of the cross section of the radial neck and the volume of the radial head for the normal and affected sides. The appearance of the radial head was classified into three types: "concave," "flat," and "domed" (Fig. 4). This evaluation was made with a 3-D bone model displayed on the computer screen by three independent reviewers (KO, TM, HM) and the type of radial head determined by consensus between at least two of the three reviewers. Changes

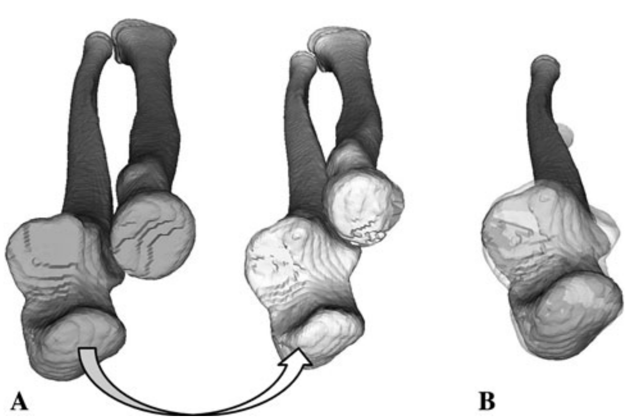

Fig. 1A–B (**A**) Mirror images of the 3-D bone models of the normal (gray) and affected (white) sides were created from CT data. (**B**) A mirror image of the normal ulna (gray) was superimposed on the affected ulna (translucent white).

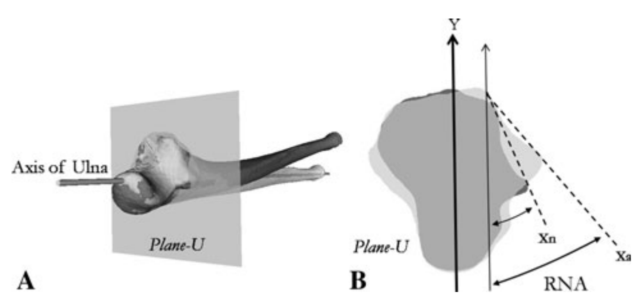

Fig. 2A–B (**A**) The plane perpendicular to the calculated axis of the ulna passing through the midpoint of the PRUJ is called "plane-U." (**B**) The RNA is the angle between the line created by joining the ends of the radial notch (normal ulna: Line Xn, affected ulna: Line Xa) and the line passing through the ulnar posterior border and the tip of the coronoid process (Line Y).

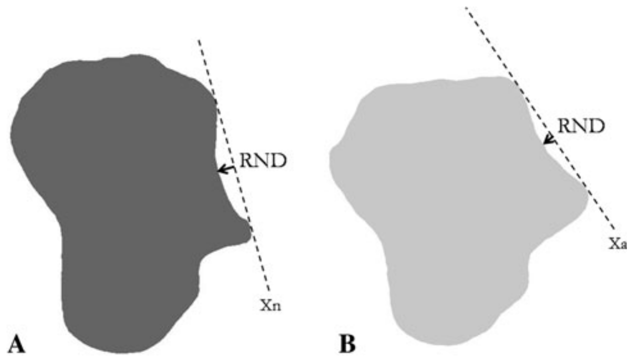

Fig. 3A–B The RND is the distance between Line X(n, a) and the bottom of the radial notch in (**A**) the contralateral normal ulna and (**B**) the affected ulna.

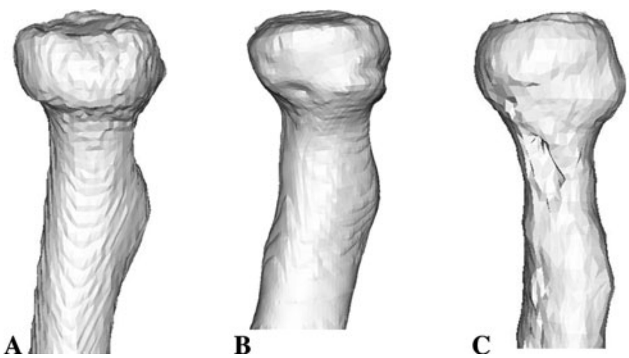

Fig. 4A–C The patterns of the morphologic features of the radial head, (**A**) concave, (**B**) flat, and (**C**) domed, are shown.

to the radial neck were evaluated by calculating the minimum transverse area of the normal (Sn) and affected (Sa) sides using a genetic algorithm on a computer [13]. Dimensional changes to the radial head were evaluated quantitatively by calculating the volume of the radial head (V) proximal to the minimal radial transverse plane (plane-S) of the normal (Vn) and affected (Va) sides (Fig. 5). Differences in minimal transverse area of the radial neck (S) and volume of the radial head (V) between the affected and normal sides (|Sn − Sa| and |Vn − Va|) relative (Rs, Rv) to the normal side (Sn, Vn) were calculated using the following equations:

$$Rs = \frac{|Sn - Sa|}{Sn} \times 100(\%) \text{ and } Rv = \frac{|Vn - Va|}{Vn} \times 100(\%)$$

Differences in values between the affected and normal sides in each group were analyzed using the paired t test. Differences in measurement values in the affected side between the early and longstanding groups were analyzed using the Mann–Whitney U test. Significance was established at $p < 0.05$.

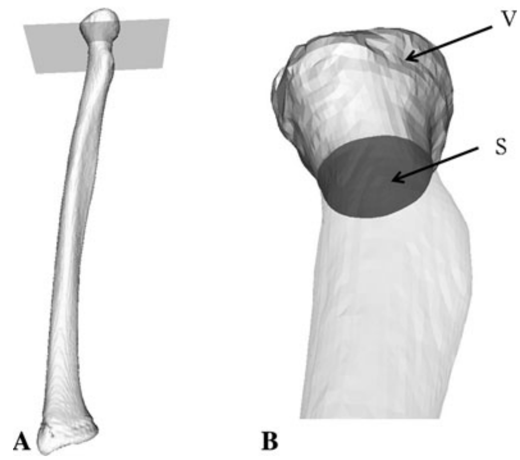

Fig. 5A–B (**A**) Plane-S is the plane at which the radial neck area is the smallest. (**B**) The minimal transverse area (S) and the volume of the radial head (V) are calculated.

Results

For the early group, the shape of the radial notch of the proximal ulna of the affected side was similar to that of the normal side. For the longstanding group, however, the radial notch was transformed in a manner corresponding to the anteriorly dislocated position of the radial head (Table 2). The average ± SD RNAs of the normal and affected sides were 25.1° ± 4.1° and 25.7° ± 4.3°, respectively ($p = 0.29$) (Fig. 6). The average RNDs of the normal and affected sides were 2.0 ± 0.8 mm and 1.6 ± 0.7 mm, respectively ($p = 0.08$) (Figs. 3A, 7). The average RNA of the normal side was 29.7° ± 6.3°, whereas that of the affected side was 45.5° ± 9.7°, indicating an increase in inclination of the radial notch ($p < 0.01$) (Fig. 6). The average RND on the normal side was 2.3 ± 1.3 mm, whereas that of the affected side (0.2 ± 1.6 mm) was smaller ($p < 0.05$) (Figs. 3, 7). The average RNA of the longstanding group was greater ($p < 0.01$) and the average RND of the longstanding group smaller ($p < 0.01$) than those of the early group.

The shape of the radial head in both groups was concave on the normal side. In the early group, two patients had a flat shape of the radial head on the affected side, whereas the remaining six patients had a concave shape of the radial head. In the longstanding group, one patient had a flat and the remaining six had dome-shaped radial heads. The average minimal transverse areas of the radial neck on the normal (Sn) and affected (Sa) sides were similar ($p = 0.43$) in the early (140 mm^2 versus 135 mm^2) and longstanding (135 mm^2 versus 127 mm^2) groups. For all the patients in the early group, the difference in cross-sectional area between the normal and affected sides relative to the normal side (Rs) was less than 20%, whereas Rs was greater than 20% in three patients in the

Table 2. Results of 3-D analysis for chronic radial head dislocations

Patient	RNA (°)		RND (mm)		Radial head shape		Area (mm^2)		Rs (%)	Volume (mm^3)		Rv (%)
	Normal	Affected	Normal	Affected	Normal	Affected	Normal (Sn)	Affected (Sa)		Normal (Vn)	Affected (Va)	
Early group												
1	24.7	27	1.7	1	Concave	Flat	137	111	19	2606	3093	18.7
2	32.8	32.4	3	2.9	Concave	Concave	179	166	7.3	5493	5636	2.6
3	27.8	26.8	3.1	1.5	Concave	Concave	137	122	10.9	3809	3873	1.7
4	24.4	25.8	2.6	2.2	Concave	Concave	174	204	17.2	5090	5990	17.7
5	21.3	19.4	1.1	0.8	Concave	Flat	78	76	2.6	591	528	10.7
6	24.2	26.3	1.7	1.6	Concave	Concave	128	134	4.7	2317	2560	10.5
7	19.2	19.9	1.7	1.8	Concave	Concave	144	128	11.1	3519	3482	1.1
8	26.4	28.3	1.4	1.3	Concave	Concave	140	137	2.1	2056	2341	13.9
Average ± SD	25.1 ± 4.1	25.7 ± 4.3	2.0 ± 0.8	1.6 ± 0.7			140	135	9.4 ± 6.4	3185	3438	9.6 ± 7.1
Long-standing group												
9	22.3	39.4	1.9	1.4	Concave	Domed	129	124	3.9	3917	3937	0.5
10	29.6	49.5	2	0.5	Concave	Domed	193	185	4.1	5590	6783	21.3
11	30.5	48.6	1.1	−0.7	Concave	Flat	90	87	3.3	1005	997	0.8
12	30.4	54.6	1.1	1.1	Concave	Domed	144	156	8.3	1677	2346	39.9
13	31.7	50.4	2	−3.1	Concave	Domed	103	77	25.2	3393	2433	28.3
14	39.7	50	4.8	0.6	Concave	Domed	173	118	31.8	6264	1245	80.1
15	23.6	26.2	3	1.3	Concave	Domed	115	141	22.6	2607	4127	58.3
Average ± SD	29.7 ± 6.3*	45.5 ± 9.7*	2.3 ± 1.3†	0.2 ± 1.6†			135	127	14.2 ± 12.0	3493	3378	32.7 ± 29.3

*Difference between normal and affected sides ($p < 0.01$); †difference between normal and affected sides ($p < 0.05$); RNA = radial notch angle; RND = radial notch depth; area = minimal cross-sectional area of radial neck; volume = radial head volume; Rs = ratio of the difference in the cross-sectional areas of the radial neck of the normal and affected sides relative to the normal side; Rv = ratio of the difference in the radial head volumes of the normal and affected sides relative to the normal side.

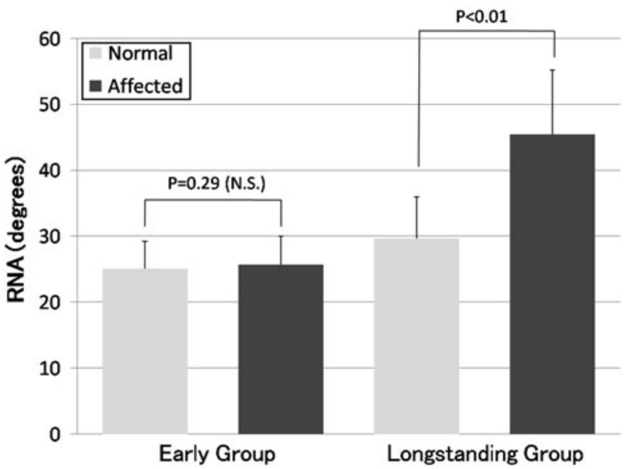

Fig. 6 No difference (p = 0.29) was observed in the RNA between the normal and affected sides in the early group. In the longstanding group, the RNA of the normal side was greater (p < 0.01) than that of the affected side because of an increase in the inclination of the radial notch. Bars = average; error bars = SD.

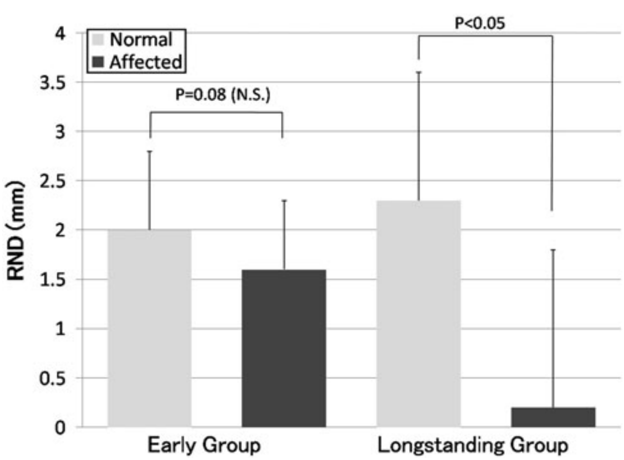

Fig. 7 No difference (p = 0.08) was observed in the RND between the normal and affected sides in the early group. In the longstanding group, the RND of the affected side was smaller (p < 0.05) than that of the normal side owing to a shallower radial notch. Bar = average; error bars = SD.

longstanding group. Regarding the volume of the radial head, the average volumes of the normal (Vn) and affected (Va) sides were similar (p = 0.0591) in the early group (3185 mm^3 versus 3438 mm^3). They also were similar (p = 0.488) in the longstanding group (3493 mm^3 versus 3378 mm^3). For the early group, the difference in radial head volume between the normal and affected sides relative to the normal side (Rv) was less than 20% in all cases, whereas that of the longstanding group was greater than 20% in five cases, indicating a marked bilateral difference. Overgrowth of the radial head by greater than 20% was observed in three cases, and undergrowth by greater than 20% was observed in two cases.

Discussion

Deformities that develop in the radiocapitellar joint and PRUJ in cases of longstanding radial head dislocation make it difficult to achieve congruent joint reduction during surgery. So far, indications for surgical intervention (in chronic radial head dislocation) included only the radiographic appearance of the radial head and humeral capitellum [11, 15, 21, 31, 32]. The PRUJ rarely has received much attention, although it is another important anatomic factor. Furthermore, it has been difficult to evaluate the PRUJ by conventional methods using plain radiographs. The aim of this study was to elucidate the 3-D morphologic changes in the PRUJ in chronic radial head dislocation using the recently developed technique of deformity evaluation with 3-D computer bone models constructed from CT data. The questions posed were: (1) What 3-D morphologic changes in the radial notch of the ulna were observed in early- versus longstanding dislocations? (2) What were the differences in the size and shape of the radial head between those two groups?

Our study had some limitations. We could not evaluate the precise shape of the surface of the articular cartilage because the 3-D model created from CT data reflected the shape of the subchondral bone and bone cortex. The numbers of patients in the early (n = 8) and longstanding (n = 7) groups were not large. Traumatic dislocations of the radial head contained various patterns of dislocation, including isolated radial head dislocations without fracture, Types I to III Monteggia lesions with ulnar fracture, and Type IV Monteggia lesions with radial and ulnar fractures.

Our results revealed the morphologic features of the radial notch were maintained in a manner relatively similar to that of the normal side in the early group less than 3 years postinjury. In contrast, the radial notch was remodeled in a manner corresponding to the dislocated position of the radial head and was substantially hypoplastic in the longstanding group more than 3 years postinjury. Consequently, notchplasty of the ulna is considered essential to reduce the dislocated radial head to the anatomic position relative to the humeral capitulum [10, 21]. However, performing notchplasty, which requires shaving intact articular cartilage of the radial notch of the proximal ulna and exposing a raw surface of cancellous bone against the radial head, is a matter of concern. We therefore recommend surgical indications be considered carefully in these cases.

For the early group, the minimal cross-sectional area of the radial neck and radial head volume showed a difference of less than 20% relative to the normal side. The appearance of the radial head was flat in two cases, with only a slight morphologic deformity observed, but it was concave in six cases, with a shape similar to normal. In the longstanding group, relative to the normal side, we observed greater than 20% overgrowth or hypoplasia of the radial head in five cases, and the appearance of the radial head was domed in six cases. If the radial head is reduced to the correct position in these cases, the deformities will prevent congruent radiohumeral and proximal radioulnar reduction and may jeopardize favorable results obtained from surgical reduction.

Our results suggested the age at which initial trauma occurred might influence remodeling of the radial notch and deformity of the radial head. In the early group, the average age of the patients at the time of the initial trauma was 9.9 years, and four patients were younger than 12 years. In the longstanding group, the average age of the patients at the time of initial trauma was 5.3 years, much younger than 8 years when the growth spurt starts [11, 21]. In the longstanding group, because the growth spurt began with the dislocation of the radial head in a nonanatomic position, the radial head may have become irreversibly overgrown or hypoplastic, and the radial notch may have remodeled in response to the dislocated radial head.

In terms of the deformation style of the radial head, as reported previously, all longstanding cases had a flat or domed shape because of the absence of pressure from the humeral capitulum [8, 11, 21, 24]. Deformation style was not consistent, and the radial head was overgrown or hypoplastic, changing with each case. These findings are thought to be contingent on the influence of peripheral soft tissue and the degree and direction of dislocation, but exact details are still unclear.

In longstanding radial head dislocation, development of deformity may be too severe in the radial head and the radial notch of the ulna to reduce the radial head to the anatomic position. It therefore is desirable to evaluate 3-D morphologic features of the radial head and radial notch with CT or MRI when the indication of open reduction for chronic radial head dislocation is determined, particularly for cases with duration of more than 3 years.

We believe the results of this study evaluating the morphologic features of the PRUJ, radial notch, and deformity of the radial head using 3-D images provides valuable information for planning therapeutic and possibly surgical strategies, and the indications for surgical intervention.

Acknowledgments We thank Ryoji Nakao, computer programmer, Department of Orthopaedic Surgery, Osaka University Graduate School of Medicine, for assistance during parts of the experimental procedure.

References

1. Audette MA, Ferrie FP, Peters TM. An algorithmic overview of surface registration techniques for medical imaging. *Med Image Anal.* 2000;4:201–217.
2. Austin R. Tardy palsy of the radial nerve from a Monteggia fracture. *Injury.* 1976;7:202–204.
3. Bado JL. The Monteggia lesion. *Clin Orthop Relat Res.* 1967;50:71–86.
4. Bell Tawse AJ. The treatment of malunited anterior Monteggia fractures in children. *J Bone Joint Surg Br.* 1965;47:718–723.
5. Besl PJ, Mackay N. A method for registration of 3-D shapes. *IEEE Trans Patt Anal.* 1992;14:239–256.
6. Best TN. Management of old unreduced Monteggia fracture dislocations of the elbow in children. *J Pediatr Orthop.* 1994;14:193–199.
7. Cappellino A, Wolfe SW, Marsh JS. Use of a modified Bell Tawse procedure for chronic acquired dislocation of the radial head. *J Pediatr Orthop.* 1998;18:410–414.
8. Exner GU. Missed chronic anterior Monteggia lesion. Closed reduction by gradual lengthening and angulation of the ulna. *J Bone Joint Surg Br.* 2001;83:547–550.
9. Fowles JV, Sliman N, Kassab MT. The Monteggia lesion in children: fracture of the ulna and dislocation of the radial head. *J Bone Joint Surg Am.* 1983;65:1276–1282.
10. Freedman L, Luk K, Leong JC. Radial head reduction after a missed Monteggia fracture: brief report. *J Bone Joint Surg Br.* 1988;70:846–847.
11. Hasler CC, Von Laer L, Hell AK. Open reduction, ulnar osteotomy and external fixation for chronic anterior dislocation of the head of the radius. *J Bone Joint Surg Br.* 2005;87:88–94.
12. Hirayama T, Takemitsu Y, Yagihara K, Mikita A. Operation for chronic dislocation of the radial head in children: reduction by osteotomy of the ulna. *J Bone Joint Surg Br.* 1987;69:639–642.
13. Holland JH. *Adaptation in Natural and Artificial Systems: An Introductory Analysis with Applications to Biology, Control, and Artificial Intelligence*. Cambridge, MA: MIT Press; 1975.
14. Holst-Nielsen F, Jensen V. Tardy posterior interosseous nerve palsy as a result of an unreduced radial head dislocation in Monteggia fractures: a report of two cases. *J Hand Surg Am.* 1984;9:572–575.
15. Horii E, Nakamura R, Koh S, Inagaki H, Yajima H, Nakao E. Surgical treatment for chronic radial head dislocation. *J Bone Joint Surg Am.* 2002;84:1183–1188.
16. Hui JH, Sulaiman AR, Lee HC, Lam KS, Lee EH. Open reduction and annular ligament reconstruction with fascia of the forearm in chronic Monteggia lesions in children. *J Pediatr Orthop.* 2005;25:501–506.
17. Hurst LC, Dubrow EN. Surgical treatment of symptomatic chronic radial head dislocation: a neglected Monteggia fracture. *J Pediatr Orthop.* 1983;3:227–230.
18. Inoue G, Shionoya K. Corrective ulnar osteotomy for malunited anterior Monteggia lesions in children: 12 patients followed for 1–12 years. *Acta Orthop Scand.* 1998;69:73–76.
19. Kadic MA, Bloem RM. Traumatic isolated anterior dislocation of the radial head: a case with a 32-year follow-up. *Acta Orthop Scand.* 1991;62:288–289.
20. Kelly DW. Congenital dislocation of the radial head: spectrum and natural history. *J Pediatr Orthop.* 1981;1:295–298.
21. Kim HT, Conjares JN, Suh JT, Yoo CI. Chronic radial head dislocation in children. Part 1: pathologic changes preventing stable reduction and surgical correction. *J Pediatr Orthop.* 2002;22:583–590.
22. Kim HT, Park BG, Suh JT, Yoo CI. Chronic radial head dislocation in children. Part 2: results of open treatment and factors affecting final outcome. *J Pediatr Orthop.* 2002;22:591–597.
23. Lichter RL, Jacobsen T. Tardy palsy of the posterior interosseous nerve with a Monteggia fracture. *J Bone Joint Surg Am.* 1975;57:124–125.
24. Lloyd-Roberts GC, Bucknill TM. Anterior dislocation of the radial head in children: aetiology, natural history and management. *J Bone Joint Surg Br.* 1977;59:402–407.

25. Lorensen W, Cline H. Marching cubes: a high resolution 3D surface construction algorithm. *Comput Graph.* 1987;21:163–169.
26. Oka K, Doi K, Suzuki K, Murase T, Goto A, Yoshikawa H, Sugamoto K, Moritomo H. In vivo three-dimensional motion analysis of the forearm with radioulnar synostosis treated by the Kanaya procedure. *J Orthop Res.* 2006;24:1028–1035.
27. Oner FC, Diepstraten AF. Treatment of chronic post-traumatic dislocation of the radial head in children. *J Bone Joint Surg Br.* 1993;75:577–581.
28. Seel MJ, Peterson HA. Management of chronic posttraumatic radial head dislocation in children. *J Pediatr Orthop.* 1999;19: 306–312.
29. Stoll TM, Willis RB, Paterson DC. Treatment of the missed Monteggia fracture in the child. *J Bone Joint Surg Br.* 1992;74: 436–440.
30. Tajima T, Yoshizu T. Treatment of long-standing dislocation of the radial head in neglected Monteggia fractures. *J Hand Surg Am.* 1995;20(3 pt 2):S91–S94.
31. Wang MN, Chang WN. Chronic posttraumatic anterior dislocation of the radial head in children: thirteen cases treated by open reduction, ulnar osteotomy, and annular ligament reconstruction through a Boyd incision. *J Orthop Trauma.* 2006;20:1–5.
32. Wilkins KE. Changes in the management of Monteggia fractures. *J Pediatr Orthop.* 2002;22:548–554.